Supplementary Material for the causal drivers of Recurrent Rossby Wave Packets

Mubashshir Ali[1,2]

[1]Institute of Geography and Oeschger Centre for Climate Change Research, University of Bern, Bern, Switzerland
[2]Moody's Risk Management Solutions Ltd, London, UK

1 Identifying RRWPs

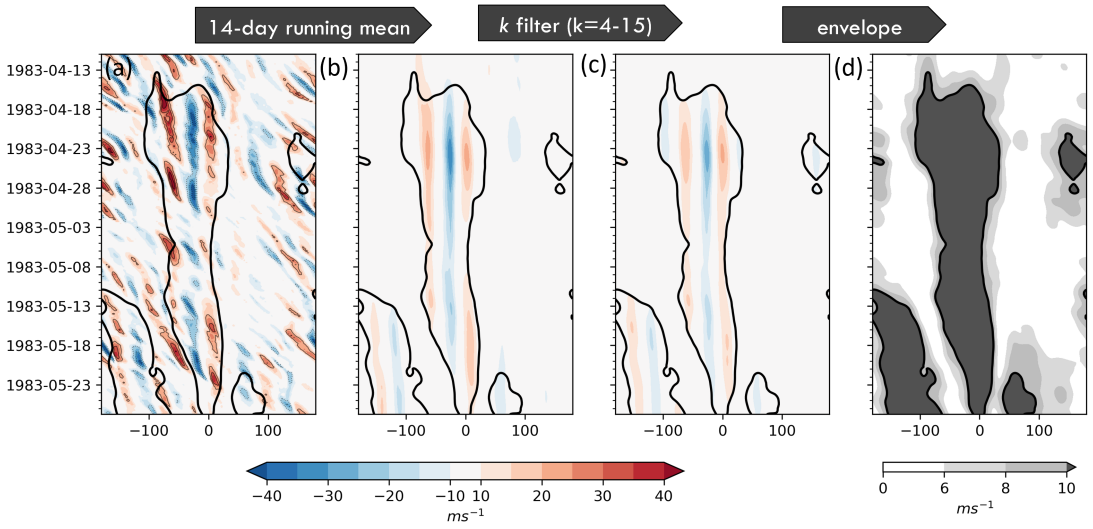

Figure 1: Computation steps for the metric R for the 1983 event. All panels show longitude vs time Hovmöller diagrams. (a) shows merdional wind at 250 hPa, v_{250} averaged between 35° and 65° N, $v_{ma(\lambda,t)}$, (b) $v_{tf}(\lambda,t)$, (c) $v_{tf,wvnf}(\lambda,t)$, and (d) $R(\lambda,t)$. Black contours in the panels show $R = 10\ ms_{-1}$ (Fig. from Ali (2022)).

Recurrent Rossby wave packets (RRWPs) are identified using the metric R (Röthlisberger et al., 2019; Ali et al., 2022, 2021). Figure 1 illustrates the steps to compute R (Ali, 2022). First, the two-dimensional meridional wind fields are averaged between 35° and 65° N at each time

step, $v_{ma(\lambda,t)}$. Then, 14.25 day running-mean fields are computed, $v_{tf}(\lambda,t)$ to smooth out high-frequency transients. Next, $v_{tf}(\lambda,t)$ is transformed into the frequency domain using a fast Fourier transform over longitude, $\hat{v}_{tf}(k,t)$. Finally, an inverse Fourier transform is applied to calculate the envelope of only the synoptic scale wavenumbers (k = 4–15), $v_{tf,wvnf}(\lambda,t)$. Thus, $R(\lambda,t)$ for each longitude λ and time t is calculated as:

$$R(l,t) = |2\sum_{k=4}^{15} \hat{v}_{tf}(k,t)e^{2\pi ikl/N}|, \tag{1}$$

2 Causal networks

Table 1: Summary of the one dimensional time series used in the CN for DJF.

Variable	Description	Grid box
R-NAt	R-metric over the North Atlantic	50°W–10°E
BU-NAt	BU over western and central Atlantic	35°–50°N, 55°W–15°W
Blocks-NAt	Fraction of area blocked over NAt	40°N–60°N, 50°W–5°W
BU-Pac	BU over Pacific	30°N–40°N, 170°E–160°W
RWS	RWS_{adv} over Pacific	20°N–40°N, 180°W–140°W

Table 2: Summary of the one dimensional time series used in the CN for JJA.

Variable	Description	Grid box
R-NAt	R-metric over North Atlantic	50°W–10°E
Blocks-NAt	Fraction of area blocked over North Atlantic	50°N–65°N, 50°W–30°W
BU-NAt	BU over North Atlantic	40°–55°N, 65°W–25°W
BU-EPac	BU over eastern Pacific	30°N–40°N, 170°W–130°W

The causal networks used in this study are based on Peter and Clark (PC) momentary conditional independence algorithm, PCMCI (Runge, 2018). An extended description of the PCMCI algorithm is provided in Di Capua et al. (2020); Kretschmer et al. (2016); Runge et al. (2019). The one dimension series used in the causal networks are summarized in tables 1 and 2 (Ali, 2022).

References

Ali, S. M.: Recurrent Rossby waves: drivers and links to persistent weather, Ph.D. thesis, Universität Bern, URL https://boristheses.unibe.ch/3756/, 2022.

Ali, S. M., Martius, O., and Röthlisberger, M.: Recurrent Rossby wave packets modulate the persistence of dry and wet spells across the globe, Geophysical Research Letters, 48, e2020GL091 452, URL https://doi.org/10.1029/2020GL091452, 2021.

Ali, S. M., Röthlisberger, M., Parker, T., Kornhuber, K., and Martius, O.: Recurrent Rossby waves during Southeast Australian heatwaves and links to quasi-resonant amplification and atmospheric blocks, Weather and Climate Dynamics Discussions, pp. 1–41, URL https://doi.org/10.5194/wcd-2022-1, 2022.

Di Capua, G., Kretschmer, M., Donner, R. V., Van Den Hurk, B., Vellore, R., Krishnan, R., and Coumou, D.: Tropical and mid-latitude teleconnections interacting with the Indian summer monsoon rainfall: a theory-guided causal effect network approach, Earth System Dynamics, 11, 17–34, URL https://esd.copernicus.org/articles/11/17/2020/, 2020.

Kretschmer, M., Coumou, D., Donges, J. F., and Runge, J.: Using causal effect networks to analyze different Arctic drivers of midlatitude winter circulation, Journal of climate, 29, 4069–4081, URL https://doi.org/10.1175/JCLI-D-15-0654.1, 2016.

Röthlisberger, M., Frossard, L., Bosart, L. F., Keyser, D., and Martius, O.: Recurrent synoptic-scale Rossby wave patterns and their effect on the persistence of cold and hot spells, Journal of Climate, 32, 3207–3226, URL https://doi.org/10.1175/JCLI-D-18-0664.1, 2019.

Runge, J.: Causal network reconstruction from time series: From theoretical assumptions to practical estimation, Chaos: An Interdisciplinary Journal of Nonlinear Science, 28, 075 310, URL https://doi.org/10.1063/1.5025050, 2018.

Runge, J., Bathiany, S., Bollt, E., Camps-Valls, G., Coumou, D., Deyle, E., Glymour, C., Kretschmer, M., Mahecha, M. D., Muñoz-Marí, J., et al.: Inferring causation from time series in Earth system sciences, Nature communications, 10, 1–13, URL https://doi.org/10.1038/s41467-019-10105-3, 2019.